Capacitive Layers Based on Lead Magnesium Niobate Buried in a Multilayer Substrate

N. Casagranda & M. Lejeune

Ecole Nationale Supérieure de Céramique Industrielle, 47 à 73 Avenue Albert-Thomas, F-87065 Limoges Cédex, France

Abstract

$0.95PbMg_{1/3}Nb_{2/3}O_3$-$0.05PbTiO_3$-$0.03PbO$ green sheets were buried in a low firing alumina package using screen-printed silver electrodes. Capacitances of $30 nF/cm^2$ with a loss tangent of 6% were obtained after co-firing at 860°C. The interaction mechanisms between the different materials were studied.

Folien aus $0.95PbMg_{1/3}Nb_{2/3}O_3$-$0.05PbTiO_3$-$0.03 PbO$ wurden im Siebdruckverfahren mit Silberelektroden versehen und in ein bei niedrigen Temperaturen verdichtendes Al_2O_3-Multilayersubstrat eingebaut. Nach dem gemeinsamen Brand bei 860°C konnte eine Kapazität von $30 nF/cm^2$ mit einem Verlustfaktor tan δ von 6% erzielt werden. Das Reaktionsverhalten der unterschiedlichen Materialien zueinander wurde untersucht.

Des bandes capacitives de composition $0.95PMN$-$0.05PT$-$0.03PbO$ ont été enterrées dans un empilement de feuilles d'alumine utilisées pour la réalisation de substrats multicouches. Aprés frittage à basse température (860°C) en présence d'électrodes d'argent, on obtient des capacités maximales de $30 nF/cm^2$ associées à des pertes diélectriques de 6%. Des études microstructurales ont permis de rendre compte des mécanismes d'intéraction entre les différents matériaux.

1 Introduction

In a hybrid microcircuit, the conductors, resistors and cross-overs are first screen-printed on to a ceramic substrate; the various chips are then surface mounted. The development of multilayer interconnecting hybrids leads to the reduction of signal propagation time, of cost and to an improvement in reliability. This kind of packaging was tested at first by IBM in the early 1980s.[1] It was made of two parts: a multilayer ceramic substrate on which the chips are mounted and a thermal conduction module.

The multilayer ceramic substrate includes many conductive levels, linked by 'vias', to provide power and to interconnect a large number of chips mounted on its upper surface. Such a structure can be achieved by thick film hybrid technology or co-fired technology.

In the case of the thick film process, the structure is built up layer by layer by consecutive printing and firing of conductive and insulating layers. The process becomes less cost effective for a large number of layers and is supplanted by co-fired technology. The high temperature co-fired technology (~ 1600°C) uses alumina as an insulating material and consequently refractory metals (Mo, W) as conductors. This technology exhibits certain disadvantages, high investment (high temperature firing in reducing atmosphere) and high resistivity of conductors. A low co-fired technology (~ 860°C) has been developed which combines the benefits of thick film (standard equipment) and co-fired technologies.[2,3] The low co-fired process uses a dielectric tape made of a silico-aluminate type compound associated with fluxing agents (K_2O, Na_2O) and silver conductors.

Moreover, innovative packaging structures are required to increase circuit density. In particular, one alternative is to integrate passive components such as resistors and capacitors to provide available area on the upper face of the circuit. So the purpose of this work is to develop ceramic dielectric compositions to be integrated as the capacitive layer in a low co-fired multilayer structure. One of the most promising dielectric materials seems to be

compositions based on lead complex perovskite compounds. In fact, these compounds are characterized by high dielectric constant (> 10 000) and low sintering temperature (< 1000°C). Moreover, the dielectric properties of $Pb(AB)O_3$ thick film capacitors are also promising.[4,5]

The material chosen for this investigation is based on the complex perovskite compound $PbMg_{1/3}$-$Nb_{2/3}O_3$ (PMN). Many previous studies have shown that the main difficulty is to avoid the presence of pyrochlore-type phases.[6,7] For that, one can use an excess of lead or magnesium oxide in the initial mixing or associate PMN with a more stable perovskite compound like $PbTiO_3$ (PT).[8,9] So, in accordance with our previous results, the composition used in this study was a 0·95PMN-0·05PT-xPbO type.

2 Experimental Procedure

2.1 Powders

The initial mixing was done according to the stoichiometries 0·95 PMN-0·05 PT-xPbO (x: 0, 3, 6 or 9 mol.%), with reagent-grade PbO (Pennaroya-Ø 50%: 7 μm- S: 1 m²/g), MgO (Léger-Lambert Rivière-Ø 50%: 6 μm- S: 27 m²/g), Nb_2O_5 (Herman Starck Ceramic Grade-Ø 50%: 0·4 μm- S: 8 m²/g) and TiO_2 (Toho-Ø 50%: 1·3 μm- S: 2·5 m²/g) attrition milled in distilled water for 1 h using zirconia balls and a dispersant (Dolapix PC 33-Zchimmer & Schwarz). The materials were calcinated at 750°C for 3 h, then crushed by an attrition process similar to the previous one. The resulting medium particle size was 0·8 μm. The relative amount of perovskite phase in the calcined powders was determined from X-ray spectra by the relation:

% Perov = I(110) Perov/I(110) Perov + I(222)Pyro

The amount of PbO evaporated during the calcination step was deduced from the weight loss of powders.

2.2 Capacitors

The capacitive part of the final multilayer structure comprises tape-cast sheets (~ 50 μm) laminated between two dielectric sheets with silver screen-printed electrodes. However, a preliminary study was carried out using disk capacitors because of the greater simplicity of the process. Granulated calcined powders corresponding to the initial compositions 0·95 PMN-0·05PT-xPbO (x: 0, 3, 6, 9%) were pressed into pellets at 100 MPa and sintered at 860°C. The sintered disk capacitors were character-

ized by the perovskite phase content determined as previously mentioned. The theoretical densities of the ceramics were then calculated from the relative amounts of phases, and the densification rate was deduced from experimental densities. The final PbO excess in the ceramics was deduced from the weight loss during sintering, added to the PbO evaporated during calcination.

The capacitance values and loss tangents were measured at 20°C with an ESI automatic capacitance bridge at 1 kHz with 1 V/rms. Direct current resistivity was measured at 1 Vdc/μm for 1 min with a Sefelec resistance meter.

Only one composition was then estimated as the capacitive layer buried in multilayer structures in view of the complexity of the process. So a composition was selected from the characteristics of the disk capacitors taking into account the following determining criteria: (i) to minimize the pyrochlore
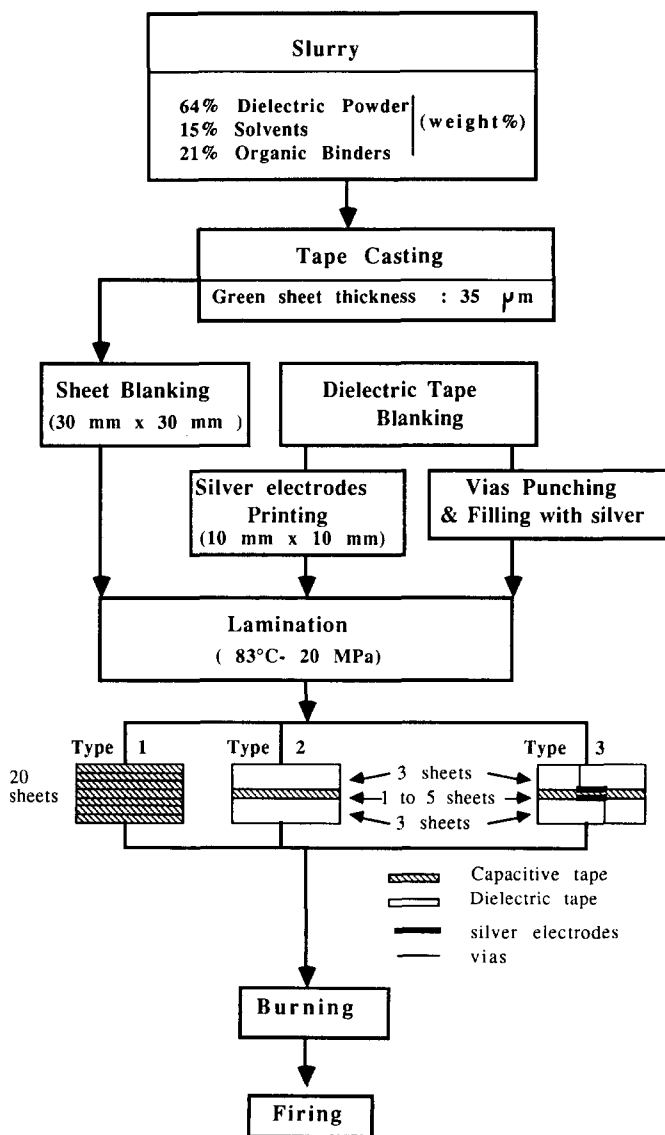

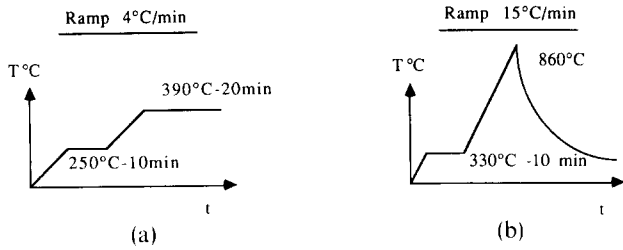Fig. 1. Process flow chart for laminated structures.

Fig. 2. Burnout (a) and firing (b) profiles for laminated structures.

content after calcination, (ii) to obtain, after sintering, a pure perovskite and densified material, (iii) with a low residual lead oxide excess. Different laminated bodies were then fabricated with the selected composition as is shown in the flow chart (Fig. 1). After casting the slurry in tape form on polypropylene film, sheets are blanked to 30 × 30 mm squares as also for the dielectric commercial tape (thickness: 114 μm-36%Al_2O_3, 48%SiO_2, 16%Na_2O-K_2O-CaO). In order to separate the respective contributions of the different constituents of the final multilayer structure, this investigation was then carried out by building successively different laminated parts (Fig. 1): (i) type 1 corresponds to a laminated structure of twenty capacitive sheets, (ii) type 2, 1–5 capacitive sheets are laminated between three dielectric sheets on both sides, (iii) finally, for type 3, silver electrodes are screen-printed on the dielectric sheets in contact with the capacitive ones, and connected to the surfaces of the laminated structure by vias, which are punched in the upper dielectric sheets and filled by silver paste. The laminated stacks are burned out in a convection oven according to the profile shown in Fig. 2(a). A conventional thick film belt furnace is then used for firing (Fig. 2(b)).

The sintered laminated structures were characterized by perovskite content, final PbO excess and densification rate. Also the linear shrinkages X, Y, Z were determined for the structure type 1 to check the compatibility with the dielectric material (shrinkage rates X, Y: 12%; Z: 17%). Cross-sections of the laminated structures types 2 and 3 were studied by electron microscopy with an Energy Dispersive Analyser (EDS) to characterize the interaction mechanisms between the different constituents. The dielectric characteristics were determined as previously mentioned for disk capacitors.

3 Results and Discussion

3.1 Disk capacitors

The microstructural and dielectric characteristics of the disk capacitors, corresponding to the initial

Table 1. Microstructural and dielectric properties of disk capacitors corresponding to 0·95PMN-0·05PT-PbO powders calcined at 750°C and sintered at 860°C.

Initial PbO excess (mol.%)	0	3	6	9
Perovskite (vol.%) calcined product	91	93	98	77
d/d_{theor} %	56	82	81	70
Perovskite (vol%)	94	99	98	99
Final PbO excess (mol%)	0	0·2	2·9	5·1
ε_r (20 C)	1050	3740	2640	1200
tg δ (20 C) × 10^2	4	2·5	3	7
ρ (10^{10} Ω cm)	3	6	1	0·5

compositions 0·95PMN-0·05PT-xPbO with x: 0, 3, 6, 9% calcined at 750 C, are listed in Table 1. An initial excess of 3 mol.% leads to the best densification rate and to a pure perovskite phase with a minimal free lead oxide, and consequently to the most interesting dielectric properties. Assuming that the evaporation mechanism of PbO in the final multilayer structures would be similar to the one noted for disk capacitors, the composition 0·95PMN-0·05 PT-0·03 PbO was selected for further investigations concerning laminated structures.
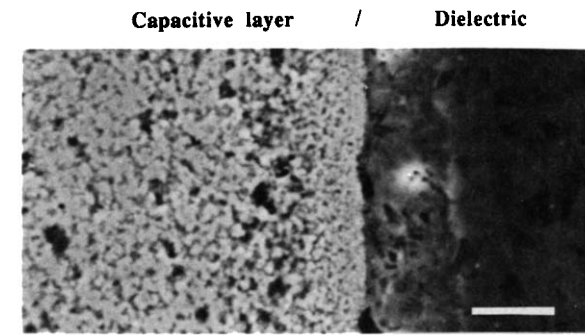
3.2 Laminated structures

The characteristics of laminated structures type 1 (Fig. 1) are listed in Table 2. As for the shrinkage X, Y, which is the most critical one, it is similar to that of the dielectric tape. Some pyrochlore phase is detected in the samples, when it was not in the disk capacitors corresponding to the same composition. In fact, the burned laminated structures have a higher porosity (52%) than the green capacitors (40%) which promotes the volatilization of PbO oxide during sintering and consequently involves the formation of the pyrochlore phase. The lower densification rate of the sintered laminated structures is also attributed to their lower initial density. Nevertheless, the dielectric properties remain compatible with the application concerned (Table 2).
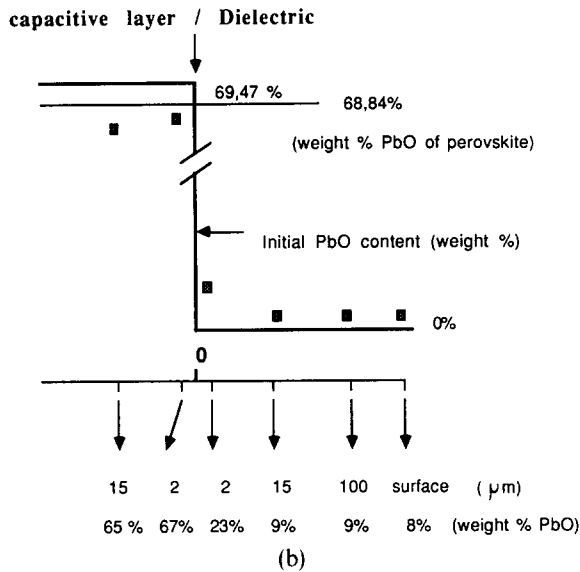
The residual PbO excess in the laminated structures type 2 (Fig. 1) ranges from 2 to 2·5% when the

Table 2. Microstructural and dielectric characteristics of a multilayer structure type 1 (20 capacitive layers, 3 mol.% initial excess PbO, calcined at 750 C)

Shrinkage X, Y	14%
Shrinkage Z	25%
Densification rate	76%
Perovskite (vol.%)	96%
Final PbO excess (mol.%)	0%
ε_r (20 C)	2700
tg δ (20 C)	2%
ρ (Ω cm)	2 × 10^{10}

Capacitive layer   /   Dielectric

(a)

capacitive layer / Dielectric

69,47 %   68,84%

(weight % PbO of perovskite)

Initial PbO content (weight %)

0%

0

15   2   2   15   100   surface   (µm)

65 % 67% 23%   9%   9%   8%   (weight % PbO)

(b)

Fig. 3. (a) Cross-section of a multilayer structure type 2 with one capacitive sheet (bar: 6 µm); (b) corresponding variation of lead oxide (■) content (wt %) determined by EDS.

number of capacitive layers increases. The result, compared to the one obtained for the structure type 1 (Table 2) suggests that the dielectric sheets tend to reduce the PbO losses. However, 20 vol.% of pyrochlore phase is detected in the capacitive area. Indeed, from the lead oxide content determined by EDS across a section of a laminated structure type 2 (Fig. 3), one can note that PbO diffuses in dielectric layers, so that the PbO content of the capacitive layers is below that of the perovskite, whereas the whole laminated structure still contains free PbO. Moreover, the interface of the capacitive layer with the dielectric material exhibits a higher PbO content than the middle layer. In fact, the PbO which is diffusing through the capacitive layer is blocked at the interface when the dielectric material is densified. This mechanism involves differences in densification rates of the capacitive layer (Fig. 3(a)).

The laminated structures type 3 differ from one another in the number of capacitive sheets ranging from 1 to 5. The dielectric properties of the different laminated structures are listed in Table 3. The dielectric permittivity of the capacitive layer in-
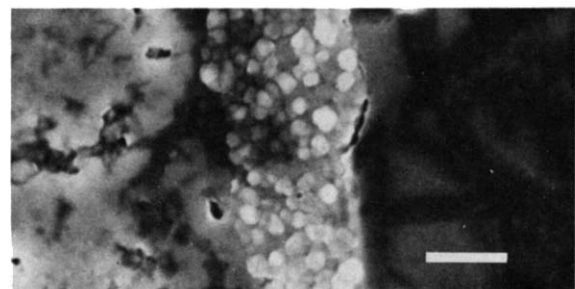
Table 3. Dielectric properties of multilayer structures type 3 versus the number of capacitive layers (3 mol.% initial excess PbO, calcined at 750°C)

Number of capacitive sheets :

1   3   5

$C(nF/cm^2)$ ε_r

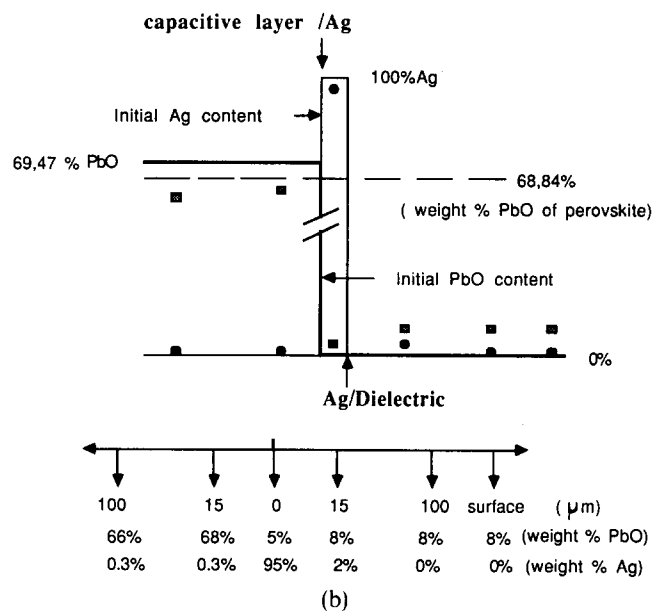| 4,7	137	27	2300	25	3500
	5%		6%		8%

$tg \, \delta$

creases with its thickness. Nevertheless, the corresponding capacitance exhibits a maximum for three capacitive sheets.

Figures 4(a) and 4(b) show respectively the cross-section of a sintered laminated structure type 3 (five capacitive layers) and the corresponding

Capacitive layer   /   Ag   /   Dielectric

(a)

capacitive layer /Ag

100%Ag

Initial Ag content →

69,47 % PbO   68,84%

(weight % PbO of perovskite)

Initial PbO content

0%

Ag/Dielectric

100   15   0   15   100   surface   (µm)

66%   68%   5%   8%   8%   8%   (weight % PbO)

0.3%   0.3%   95%   2%   0%   0%   (weight % Ag)

(b)

Fig. 4. (a) Cross-section of a multilayer structure type 3 with five capacitive sheets (bar: 2 µm); (b) corresponding variation of lead oxide (■) and Ag (●) contents (wt %) determined by EDS.

variations of PbO and silver contents. So the variation of the dielectric permittivity of the capacitive layer with its thickness can be attributed to the diffusion of the PbO in the dielectric material through the silver electrode. Indeed this mechanism involves a lack of PbO and, consequently, the development of the pyrochlore phase, all the greater as the capacitive layer is thin. Moreover, significant crystallization can be observed in Fig. 4(a) at the dielectric–silver electrode boundary. According to the EDS results, these crystallites are identified as $PbO-2CaO$. They are presumed to grow at $822°C$ during the cooling step in a liquid phase resulting from the reaction of the lead oxide with the fluxing agent of the dielectric material. On the other hand, no silver diffusion from electrodes has been detected.

4 Conclusion

$0·95PMN-0·05PT-0·03PbO$ capacitive sheets were buried in a multilayer low-firing alumina structure with silver screen-printed electrodes. The resultant package exhibits a capacitance of $30\,nF/cm^2$ and loss tangent of 6% after co-firing at $860°C$. So materials based on the $0·95PMN-0·05PT$ system seems very promising for applications as decoupling capacitors in multilayer ceramic interconnection packages and more widely in monolithic multicomponent ceramic substrates.[10] However, it seems absolutely necessary to minimize the diffusion of PbO in the structure because, in spite of correct instantaneous dielectric properties, the material can show a poor stability with time. So it would be interesting to test the potential of the same system

with addition of MgO instead of PbO. In fact, previous studies have shown that addition of MgO allows an increase in the stability of perovskite phase; however, such excess would have to be minimized because of the simultaneous increase in the sintering temperature. A comparison of results obtained for PbO or MgO excess will allow us to determine which is the most adequate.

References

1. Blodgett, A. J. & Barbour, D. R., Thermal conduction module: a high-performance multilayer ceramic package. *IBM J. Res. Dev.*, **26**(1) (1982) 30–6.
2. Eustice, A. L. & Nishii, N., Low temperature co-fireable ceramics for multilayer interconnect hybrids. *IMC Proceedings*, Kobe, May 1986.
3. Steinberg, J. I., Development of a low temperature cofired multilayer ceramic technology. *ISHM* (1985).
4. Shen-Li Fu & Gung-Fu Chen, Low temperature firing $Pb(Fe_{2/3}W_{1/3})_x(Fe_{1/2}Nb_{1/2})_yTi_zO_3$-based thick film capacitors materials. *Proc. Int. Symp. Micro.*, 1985.
5. Reiley, T. C. & Badding, J. V., A low-temperature firing thick film capacitor material based on lead iron niobate tungstate. *Mater. Res. Bull.*, **19** (1984) 1543–9.
6. Swartz, S. L. & Shrout, T. R., Fabrication of perovskite lead magnesium niobate. *Mater. Res. Bull.*, **17** (1982) 1245–50.
7. Goo, E., Microstructure of lead-magnesium niobate ceramics. *J. Am. Ceram. Soc.*, **69**(8) (1986) C-188–190.
8. Halliyal, A., Guruja, T. R., Kumar, U. & Safari, A., Stability of perovskite phase in $Pb(Zn_{1/3}Nb_{2/3})O_3$ and other $A(B'B'')O_3$ perovskites. *IEEE International Symposium on application of ferroelectrics*, Bethlehem, 1986.
9. Boilot, J. P., Bouquin, O. & Lejeune, M., Compositions diélectriques à basses températures de frittage à base de niobate de plomb et de magnésium. *Silicates Industriels Ceramic Science Technology*, 1–2 (1990) 27–32.
10. Utsumi, K., Shimada, Y., Ikeda, T. & Takamizawa, H., Monolithic multicomponents ceramic substrate. *Ferroelectrics*, **68** (1986) 157–79.